

## Lamb-shift and fine-structure measurements in ${}^7\text{Li}^+$

R. A. Holt, S. D. Rosner, T. D. Gaily, and A. G. Adam

*Department of Physics, University of Western Ontario, London, Ontario N6A 3K7, Canada*

(Received 24 March 1980)

We have measured the absolute wave numbers of the  $2s\ {}^3S_1$ - $2p\ {}^3P_J$  transitions in  ${}^7\text{Li}^+$  by laser fluorescence spectroscopy on an ion beam. Using the hyperfine structure (hfs) theory of Jette, Lee, and Das, we have extracted the following hfs-free wave numbers:  $\sigma(2s\ {}^3S_1$ - $2p\ {}^3P_0)$  = 18 231.3030(12),  $\sigma(2s\ {}^3S_1$ - $2p\ {}^3P_1)$  = 18 226.1082(12), and  $\sigma(2s\ {}^3S_1$ - $2p\ {}^3P_2)$  = 18 228.1979(12)  $\text{cm}^{-1}$ . By subtracting the theoretical values of Accad, Pekeris, and Schiff, we obtain the differential Lamb shifts  $S(2s\ {}^3S_1$ - $2p\ {}^3P_0)$  = 1.2539(16),  $S(2s\ {}^3S_1$ - $2p\ {}^3P_1)$  = 1.2543(16), and  $S(2s\ {}^3S_1$ - $2p\ {}^3P_2)$  = 1.2545(16)  $\text{cm}^{-1}$ . These results are in agreement with the calculations of Ermolaev and with earlier measurements by Bacis and Berry. The fine-structure intervals obtained from the absolute wave numbers are in agreement with the theory of Accad *et al.* and with the measurements of Bacis and Berry, but they exhibit a disagreement, which amounts in one case to two standard deviations, with the recent more precise results of zu Putlitz and co-workers.

### I. INTRODUCTION

The Lamb shift, fine structure (fs), and hyperfine structure (hfs) in the spectrum of  $\text{Li}^+$ , the second member of the helium isoelectronic sequence, have been studied extensively over the years.<sup>1-14</sup> In contrast to the hydrogenic case, the excited states of a given principal quantum number are far from degenerate, making it impossible to measure the Lamb shift by microwave techniques. In spite of this, the experimental accuracy<sup>8</sup> is currently superior to that of the theoretical calculations.<sup>15</sup> The major obstacle for theorists is not the lack of accurate nonrelativistic wave functions, which have been available for some time<sup>16</sup>; the central problem is the difficulty in carrying out two-electron oscillator-strength sums over all discrete and continuum states of the ion.<sup>15</sup> The development of consistent and sophisticated methods for the inclusion of quantum electrodynamic effects in calculations on two-electron atoms would be a major step forward in the theory. It has already been shown in the case of He that the theory can be advanced to the point that a fine-structure measurement on a two-electron atom can yield a measurement of the fs constant  $\alpha$  to better than 1 ppm, which is more accurate than the value of  $\alpha$  derived from hydrogen fs measurements.<sup>17</sup> Recent measurements of the Lamb shift, fs, and hfs in  $\text{Li}^+$  have generated an urgent need for further theoretical progress.

In the present paper we will describe a new experiment which significantly improves our knowledge of the differential  $2s\ {}^3S_1$ - $2p\ {}^3P_J$  Lamb shifts in  ${}^7\text{Li}^+$  and which adds some useful information concerning the serious discrepancy between the experimental and theoretical values of the  $2p\ {}^3P_J$  fs intervals.<sup>14</sup> Briefly, the measurement carried

out was a determination of the absolute wave numbers of the  $2s\ {}^3S_1$ - $2p\ {}^3P_J$  transitions at 548.5 nm (see Fig. 1) using laser fluorescence spectroscopy on a Doppler-tuned ion beam. An important new averaging technique was introduced which allowed the wave numbers to be measured to an accuracy of 0.0012  $\text{cm}^{-1}$  and eliminated the need for accurate knowledge of the ion-beam energy. With the aid of the fs and hfs calculations to be described in the following section, these measurements enabled us to determine the differential Lamb shifts to an accuracy of 0.0016  $\text{cm}^{-1}$ .

### II. THEORY

The most accurate calculations of the  $\text{Li}^+ 2s\ {}^3S_1$ -

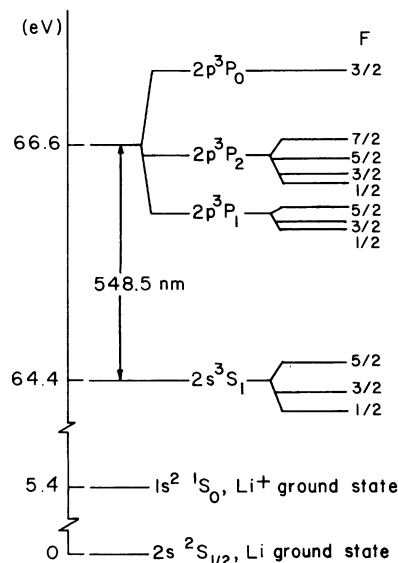


FIG. 1. Partial Grotrian diagram of  ${}^7\text{Li}^+$  showing the levels investigated.

$2p\ ^3P_1$  interval are those of Accad, Pekeris, and Schiff (APS).<sup>16,18</sup> Accurate nonrelativistic wave functions were obtained by a variational calculation employing a triple series of Laguerre polynomials of the perimetric coordinates (linear combinations of the distances of the two electrons from the nucleus and the interelectronic distance), thus effectively including the correlation effects which are quite important for  $n=2$  states. Relativistic effects up to order  $\alpha^2$  were added by perturbation theory, as was the mass-polarization correction for the finite mass of the nucleus. They also computed the fs intervals to order  $\alpha^3$ . Neither the Lamb shift nor the effect of singlet-triplet mixing were included in the original calculation. The importance of the latter was emphasized by Ermolaev and Jones,<sup>19</sup> and the resulting shift of the  $2p\ ^3P_1$  level was computed by them and by APS.<sup>18</sup> At the present time, then, the best theoretical estimates of the transition wave numbers excluding radiative corrections are<sup>16,18</sup>

$$\sigma(0) = 18\ 232.5569(10)\ \text{cm}^{-1},$$

$$\sigma(1) = 18\ 227.3625(10)\ \text{cm}^{-1},$$

$$\sigma(2) = 18\ 229.4524(10)\ \text{cm}^{-1},$$

where  $\sigma(J)$  is the wave number of the  $2s\ ^3S_1$ - $2p\ ^3P_J$  transition.

The earliest calculation of the order  $\alpha^3$  radiative corrections to the  $2s\ ^3S_1$  energy was Dalgarno's estimate<sup>20</sup>:

$$E_L = 1.14(10)\ \text{cm}^{-1}.$$

(Note that some authors state the shift of the ionization potential; this differs by a sign from the energy-level shifts we list.) Berry and Bacis<sup>6</sup> extrapolated the He calculations of Suh and Zaidi<sup>21</sup> to obtain

$$E_L = 0.99(4)\ \text{cm}^{-1}.$$

They had made a preliminary measurement<sup>6</sup> of the  $2s\ ^3S_1$ - $2p\ ^3P_1$  differential Lamb shift, obtaining<sup>22</sup>

$$\delta(2s\ ^3S_1 - 2p\ ^3P_1) = 1.274(15)\ \text{cm}^{-1},$$

and they suggested that the large discrepancy was due to an unexpectedly large negative shift of the  $2p\ ^3P_1$  level. Ermolaev has calculated<sup>15</sup> the shifts of both levels, showing that indeed the  $2p\ ^3P_1$  level has a Lamb shift which is nearly two orders of magnitude greater than the value  $\pm 0.007\ \text{cm}^{-1}$  expected for a  $2p$  electron in a  $Z=2$  hydrogenic ion. The major contribution to  $E_L(2p\ ^3P_1)$  comes from the electron density term  $\delta E_1$ , which is proportional to the electron correlation function. For the  $n\ ^3P$  states, but not the  $n\ ^1P$  ones, the correlation is quite substantial and negative: The electron density at the nucleus is lower than in the  $|1s\rangle$  state of the hydrogenic ion. A second contrib-

ution to  $E_L$  is  $\delta E_2$ , a sum of terms involving electric-dipole oscillator strengths between the given state and all other states of the ion. Ermolaev has computed this by an effective-oscillator-strength-sum method employing simple wave functions; the same method applied to He gives results in reasonable agreement with the direct summation by Suh and Zaidi.<sup>21</sup> The uncertainty in the term  $\delta E_2$  is estimated to be  $\pm 0.040\ \text{cm}^{-1}$  in the case of  $2s\ ^3S_1$  and  $\pm 0.037\ \text{cm}^{-1}$  for  $2p\ ^3P_1$ . Altogether, Ermolaev calculates

$$E_L(2s\ ^3S_1) = 1.025(55)\ \text{cm}^{-1},$$

$$E_L(2p\ ^3P_1) = -0.291(41)\ \text{cm}^{-1}.$$

In any actual measurement on  $\text{Li}^+$  one must deal with the additional complication of hyperfine structure. The hfs splittings are only an order of magnitude smaller than the fine structure, so that levels of the same  $F$  but different  $J$  are mixed. Jette, Lee, and Das<sup>23</sup> have carried out a linked-cluster many-body perturbation calculation of the  $2p\ ^3P$  hfs. Their work has been confirmed to  $\pm 0.0003\ \text{cm}^{-1}$  by a variety of experimental techniques,<sup>12-14,24</sup> and we have also measured the hyperfine intervals by the same method used by Lurio and co-workers,<sup>12,13</sup> with results in good agreement. Thus we conclude that the hfs is well understood at the level of precision ( $\pm 0.001\ \text{cm}^{-1}$ ) aimed at in the Lamb shift and fs measurements to be described below. In order to extract a Lamb-shift value from the measured wave number of a particular hyperfine component, we first obtain the hypothetical interval  $\sigma(J)$  that would exist in the absence of hfs, using the theoretical hfs energies of Jette, Lee, and Das. This can then be compared directly with a  $2s\ ^3S_1$ - $2p\ ^3P_J$  interval calculated by APS to yield a Lamb shift.

### III. EXPERIMENTAL METHOD

Laser fluorescence spectroscopy on a Doppler-tuned ion beam has been used by several groups,<sup>12,13,25-27</sup> principally because of the narrow optical linewidths<sup>28</sup> and the relative ease with which the frequency scale may be calibrated. However, unless small frequency intervals are being measured, the ultimate limit on the accuracy of such experiments is usually the precision with which the ion-beam energy can be measured. This energy is not simply related to the accelerating voltage because of ion-source plasma potentials, unknown potential distributions within the source, contact potentials, and charging of surfaces within the vacuum chamber. We have developed a method which yields absolute wave numbers to  $\pm 0.001\ \text{cm}^{-1}$  without precise knowledge of the absolute ion-beam energy. It requires a minimum of two mea-

surements to determine a wave number, and the ion-beam energy must remain very stable during these measurements. Consider an ion beam and a laser beam traveling in opposed directions at an angle  $\theta$ , and superimposed over some region (see Fig. 2). In order to achieve resonance with an optical transition at frequency  $\nu_0$  in the ion's rest frame, the laser frequency  $\nu_l$  will have to be set to a frequency  $\nu_l = \nu_a < \nu_0$  because of the blue Doppler shift. For a given beam energy  $E_a$  the resonance condition is given by the relativistic Doppler formula

$$\nu_0 = \gamma_a(1 + \beta_a \cos\theta) \nu_a, \quad (1)$$

in which  $\beta_a = v_a/c \approx (2E_a/Mc^2)^{1/2}$ ,  $\gamma_a = (1 - \beta_a^2)^{-1/2}$ , and  $M$  is the ionic mass. If the laser beam is reflected precisely back on itself, resonance can also be achieved at a new laser frequency  $\nu_l = \nu_b > \nu_0$ , using the red Doppler shift of the retroreflected beam. For this case,

$$\nu_0 = \gamma_b(1 - \beta_b \cos\theta) \nu_b, \quad (2)$$

and we can always choose  $\nu_a$  and  $\nu_b$  so that resonance occurs at approximately the same beam energy  $E_a \approx E_b$ . Equations (1) and (2) may readily be solved for  $\nu_0$  by eliminating  $\cos\theta$ , yielding

$$\nu_0 = \gamma_a \gamma_b (\beta_a + \beta_b) / (\gamma_b \beta_b / \nu_a + \gamma_a \beta_a / \nu_b). \quad (3)$$

This expression is remarkably insensitive to variations of both  $E_a$  and  $E_b$  by the *same* amount, corresponding to an uncertainty in the absolute ion-beam energy. Thus, if we let  $E_a = E_a^{(0)} + \Delta E$  and  $E_b = E_b^{(0)} + \Delta E$ , we find for typical experimental parameters that  $d\nu_0/dE \approx 5 \times 10^{-6} \text{ cm}^{-1}/\text{eV}$ . In fact, it is easy to see from Eq. (3) that  $\nu_0$  is entirely independent of  $E_a, E_b$  in the special case  $E_a = E_b$ . We show in Eq. (9) below that the energies  $E_a$  and  $E_b$  really enter in the form  $E_a^{1/2} - E_b^{1/2}$ , in first order, and this expression can be determined much more precisely than  $E_a$  or  $E_b$ .

For historical reasons<sup>29</sup> we chose an ion-beam-

laser-beam intersection angle  $\theta \approx 11^\circ$  rather than collinear geometry (see Fig. 2). A cw-dye-laser beam passes through a fiducial aperture  $S_1$ , intersects a  $\text{Li}^+$  beam, passes through a second aperture  $S_2$ , and is then reflected upon itself, using  $S_1$  and  $S_2$  to guarantee accurate alignment. The laser power was typically 8–15-mW single mode, spread over a diameter of 4 mm by a beam expander and a spatial filter. An isolator was used to prevent the return beam from entering the laser and causing instabilities. In practice it was also necessary to deviate the return beam by about 0.4 mrad in the direction perpendicular to the plane of intersection of the laser and ion beams. This angle adds in quadrature with  $\theta$  and has a negligible effect.

The laser frequency was stabilized and measured by locking it to a suitably chosen  $\text{I}_2$  absorption line, whose centroid wave number is known absolutely to  $\pm 0.001 \text{ cm}^{-1}$  from the work of Luc and Gerstenkorn.<sup>30,31</sup> Although it is possible to achieve a conventional first derivative lock to the peak of the  $\text{I}_2$  line using a jitter applied to the laser cavity mirror, such a lock proved too unstable for the desired precision. The  $\text{I}_2$  lines are superpositions of many hfs components, resulting in marked asymmetry near the peak of the even- $J$  lines and very flat tops for the odd- $J$  lines. The effect of this was excessive drift and uncertainty in the laser frequency. Furthermore, the centroid and the peak absorption frequency do not coincide, so that an understanding of the  $\text{I}_2$  line shape is necessary in any case. Consequently, we chose to lock the laser cavity sequentially to the half-maximum-absorption points of a chosen  $\text{I}_2$  line using the dc-ratio method.

The details of the laser lock were as follows. A portion of the laser light was picked off and passed through a beamsplitter; half went directly to a Si photodiode (B in Fig. 2), and the other half traversed an insulated room-temperature  $\text{I}_2$  absorp-

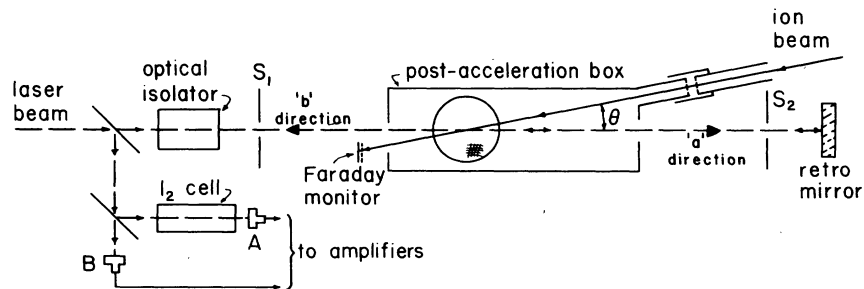


FIG. 2. Schematic diagram of the apparatus. A photomultiplier views the intersection region through the circular mesh on top of the postacceleration box.

tion cell before striking a second photodiode (A). After separate amplification of the two photocurrents  $I_A$  and  $I_B$ , the ratio  $I_A/I_B$  was formed by an analog divider. This ratio is proportional to the transmittance of the  $I_2$  cell, independent of laser amplitude fluctuations. In order to suppress spurious variations of this ratio arising from laser pointing instability, the direction of the input beam to the  $I_2$  system was narrowly defined by a pair of 2-mm apertures separated by about 70 cm. The divider output was compared with a preset reference voltage  $V_{ref}$ ; the difference, after further amplification with a 0.22-sec time constant, served as the correction signal for locking the laser cavity mode to the side of the  $I_2$  line. Depending on the desired side of the  $I_2$  line, the correction signal was inverted or not, and then fed to the cavity auxiliary input of a Spectra-Physics 481A laser controller to complete the loop. A second loop locked the laser's mode-selecting étalon to the cavity mode using a conventional first derivative lock with a 1-kHz jitter applied to the étalon's piezoelectric transducer. By varying  $V_{ref}$ , the laser could be locked to any chosen point on an  $I_2$  line with a maximum excursion of  $\pm 2.5 \times 10^{-4} \text{ cm}^{-1}$  for the weaker lines, and  $\pm 1.0 \times 10^{-4} \text{ cm}^{-1}$  for the strongest, over the time taken to accumulate a complete spectrum. The laser FM noise outside the band-pass of the loop was inconsequential in view of the 0.1-sec dwell time of the multichannel analyzer (MCA) used to record the spectra.

The ion beam was produced by a low-pressure oscillating-electron-bombardment ion source locally designed and constructed. It produced typically 100 nA of  ${}^7\text{Li}^+$  at the laser intersection, some 1.7 m downstream. Roughly 3% of the ions were in the  $2s\,{}^3S_1$  metastable level, a very significant improvement over previous experiments.<sup>12-14</sup> A full description of the source will be given elsewhere.<sup>32</sup> The ion beam was accelerated to energies in the range of 4100–6300 eV and mass-selected by a Wien-type mass filter. At the entrance to the scanning box (see Fig. 2) the ion beam was further accelerated as it passed between a pair of closely spaced grids oriented perpendicularly to the ion velocity in order to avoid deflection of the beam. The scan box voltage at resonance was typically –450 V.

In a typical experiment, the laser was locked first to  $\nu_a^L$ , the low-frequency half-point of the  $I_2$  line chosen for the “a” measurement. The ion-beam energy was then scanned by varying the potential applied to the postacceleration box surrounding the interaction region. The laser-induced fluorescence emitted into a cone perpendicular to the plane of intersection was viewed by a cooled photomultiplier, and a spectrum was accumulated

by recording the photocurrent versus scan voltage on the MCA. The MCA's channel-advance pulses were counted by a scaler whose output was processed by a D/A converter to produce a staircase scan voltage. After amplification the staircase voltage was added to a dc pedestal voltage and applied to the postacceleration box. The calibration of the scan voltage versus channel number was checked before and after each spectrum, and was stable and accurate to better than 0.01%. Depending on the signal-to-noise ratio, between 5 and 20 scans at 0.1-sec/channel, were required to obtain a spectrum. This procedure was then repeated with the laser locked to  $\nu_a^L$ ,  $\nu_b^L$ , and  $\nu_b^H$ , where the superscripts (L,H) refer to the (low, high) frequency sides of the  $I_2$  lines, whose centroids are  $\nu_a (< \nu_0)$  and  $\nu_b (> \nu_0)$ . To obtain an experimental measure of ion-beam-energy drift over the course of the measurements, the laser was returned to the  $a$   $I_2$  line and the  $\nu_a^L$  and  $\nu_a^H$  runs were repeated. Thus, each experiment produced six spectra in the sequence  $a$ - $b$ - $a$ , or occasionally  $b$ - $a$ - $b$ .

#### IV. DATA ANALYSIS

A typical fluorescence spectrum is shown in Fig. 3 for a peak energy of 5.5 keV; the calibration is approximately 1.2 eV/channel. The resonance line shape is determined primarily by the energy distribution of the ion beam; the overall width of the line arises from energy spread and angular divergence of the ion beam in roughly comparable amounts. In the spectrum shown the full width at half maximum (FWHM) is 15 eV, corresponding to an optical resolution of 950 MHz, and the shape is noticeably asymmetrical, as has been observed by other workers.<sup>12,13</sup> In order to extract a single

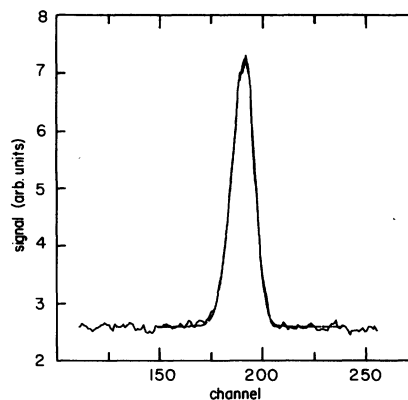


FIG. 3. A sample fluorescence spectrum, showing the  $\frac{5}{2} \rightarrow \frac{3}{2}$  component of the  $2s\,{}^3S_1$ - $2p\,{}^3P_0$  transition, at a beam energy of 5.5 keV. Total data accumulation time is 0.5 sec/channel. The dotted line is the least-squares fit.

number which characterizes the position of the peak of the line, we made a least-squares fit to an asymmetrical Gaussian plus a background:

$$C(N) = A \exp[-(N - N_0)^2/\gamma^2] + B,$$

where

$$\gamma = \begin{cases} \gamma_L, & N < N_0 \\ \gamma_R, & N > N_0. \end{cases}$$

Here,  $C(N)$  is the number of counts in channel  $N$ , and the fitted parameters are  $A$ ,  $B$ ,  $N_0$ ,  $\gamma_L$ , and  $\gamma_R$ . The exact shape of the curve is of no importance; the method relies on the fact that the fitted parameter  $N_0$  is related to the "true center" of the line (in the hypothetical situation of no Doppler width) in the *same* way for each of the four choices  $\nu_a^L$ ,  $\nu_a^H$ ,  $\nu_b^L$ , and  $\nu_b^H$  discussed above.

The  $N_0$  values were converted to beam energies using the scan calibrations; the final beam energy  $E$  for a given  $N_0$  was the sum of the total voltage on the box and the acceleration voltage applied between the ion source and ground. The latter was measured to 0.1% accuracy. Over the complete set of data, the rms drift of  $E$  between the first pair and last pair within a set of six measurements was 1.1 V. Several runs in which the drift was substantially greater than this were not included in the data analyzed; these larger drifts generally resulted when the source had not been conditioned by running it for sufficient time following a lithium reloading. The repeated value of  $E_a^L$  or  $E_a^H$  was averaged with the original one, so that a set of six spectra produced four peak positions  $E_a^L$ ,  $E_a^H$ ,  $E_b^L$ , and  $E_b^H$ , from which the wave number of a single  $\text{Li}^+$  transition was extracted.

The extraction of the  $\text{Li}^+$  wave numbers was complicated by the fact that the spectra were taken with the laser set to half-maximum-absorption points of  $I_2$  lines, whereas it is the centroids of these lines which are known. From the measured hfs constants of Levenson and Schawlow,<sup>33</sup> it is possible to model accurately the line profile of a given rotational component of the  $I_2$   $B-X$  transition, using the summed absorption coefficients of the various hfs components. A detailed discussion of the  $I_2$  line shape is given in the Appendix. From such a model, the position of the centroid  $\nu$  relative to the half-maximum-absorption points can be calculated; this is expressed by a parameter

$$r = (\nu - \nu^L)/(\nu^H - \nu^L). \quad (4)$$

A completely symmetric line would have  $r = 0.5$ . Even though the  $r$  values were accurately calculated for the known hfs, it is important to note that they are only weakly dependent on these parameters. As is shown in the Appendix, the uncertainties in the hfs and in the measured trans-

mission lead to errors in determining the centroid which are no larger than  $4 \times 10^{-5} \text{ cm}^{-1}$ .

In order to express the  $\text{Li}^+$  resonance frequency  $\nu_0$  in terms of experimentally determined quantities, we first apply Eq. (1) to the cases  $\nu_i = \nu_a^L$  and  $\nu_i = \nu_a^H$  to obtain

$$\nu_0/\nu_a^L = \gamma_a^L(1 + \beta_a^L \cos\theta_a^L) \quad (5a)$$

and

$$\nu_0/\nu_a^H = \gamma_a^H(1 + \beta_a^H \cos\theta_a^H). \quad (5b)$$

As can be seen from Eq. (4), the centroid  $\nu$  is the weighted average of  $\nu^L$  and  $\nu^H$ ; in particular, for case  $a$ ,

$$\nu_a = (1 - r_a)\nu_a^L + r_a\nu_a^H.$$

Furthermore, because  $\nu_a^H - \nu_a^L \ll \nu_a$ , we have the excellent approximation

$$1/\nu_a \approx (1 - r_a)/\nu_a^L + r_a/\nu_a^H,$$

with a fractional error of less than  $10^{-12}$ . Thus we have from Eqs. (5):

$$\nu_0/\nu_a = \langle \gamma_a + \gamma_a \beta_a \cos\theta_a \rangle, \quad (6)$$

in which the brackets  $\langle \rangle$  indicate the weighted average, e.g.,

$$\langle \gamma_a \rangle = (1 - r_a)\gamma_a^L + r_a\gamma_a^H.$$

For case "b" we obtain a similar expression,

$$\nu_0/\nu_b = \langle \gamma_b - \gamma_b \beta_b \cos\theta_b \rangle. \quad (7)$$

Assuming that  $\theta_a^L = \theta_a^H = \theta_b^L = \theta_b^H = \theta$ , we can eliminate  $\cos\theta$  to yield the generalized form of Eq. (3):

$$\nu_0 = \frac{\langle \gamma_a \rangle \langle \gamma_b \beta_b \rangle + \langle \gamma_b \rangle \langle \gamma_a \beta_a \rangle}{\langle \gamma_b \beta_b \rangle / \nu_a + \langle \gamma_a \beta_a \rangle / \nu_b}. \quad (8)$$

To display explicitly the first-order dependence of  $\nu_0$  on energy and angle, we set  $\gamma_a = \gamma_b = 1$  in Eqs. (6) and (7) and combine the resulting equations to give

$$\nu_0 \approx \nu^* \left[ 1 + \frac{1}{2} (\langle \beta_a \cos\theta_a \rangle - \langle \beta_b \cos\theta_b \rangle) \right], \quad (9)$$

where

$$\nu^* \equiv 2\nu_a \nu_b / (\nu_a + \nu_b).$$

Suppose that all four beam energies that go into the calculation of  $\nu_0$  are shifted by the same amount  $\Delta E$ . From Eq. (9) we find

$$\frac{d\nu_0}{dE} = \frac{\partial \nu_0}{\partial E_a^L} + \frac{\partial \nu_0}{\partial E_a^H} + \frac{\partial \nu_0}{\partial E_b^L} + \frac{\partial \nu_0}{\partial E_b^H} \quad (10a)$$

$$\approx (\nu^*/2Mc^2) (\langle \beta_a^{-1} \cos\theta_a \rangle - \langle \beta_b^{-1} \cos\theta_b \rangle) \quad (10b) \\ = 5 \times 10^{-6}$$

in  $\text{cm}^{-1}/\text{eV}$  for typical experimental parameters. Thus even a  $\Delta E$  of 100 eV produces a change in  $\nu_0$  of only  $5 \times 10^{-4} \text{ cm}^{-1}$ . Consider, however, the

sensitivity of  $\nu_0$  to a change in *one* of  $\langle E_a \rangle$  or  $\langle E_b \rangle$ , as represented by the first or second term of Eq. (10b):

$$\frac{d\nu_0}{d\langle E_a \rangle} \approx \left( \frac{\nu^*}{2Mc^2} \right) \langle \beta_a^{-1} \cos\theta_a \rangle = 1.2 \times 10^{-3} \quad (11)$$

in  $\text{cm}^{-1}/\text{eV}$ . This number gives an indication of the errors to be expected from drifts in ion-source potentials during a set of measurements. We deal with such drifts by making *a-b-a* or *b-a-b* sequences of measurements, as discussed earlier, and by averaging data from different days to further reduce the effect of small drifts. Note also from Eq. (11) that  $\nu_0$  becomes less sensitive to these drifts at higher ion-beam energies.

To see the effect of angular drifts, suppose  $\langle \theta_a \rangle$  differs by an amount  $\Delta\theta_a$  from  $\langle \theta_b \rangle$ . From Eq. (9) we have

$$\frac{d\nu_0}{d\langle \theta_a \rangle} = \frac{\partial\nu_0}{\partial\theta_a^L} + \frac{\partial\nu_0}{\partial\theta_a^H} \quad (12a)$$

$$\approx -\frac{1}{2}\nu^* \langle \beta_a \sin\theta_a \rangle = 2.3 \times 10^{-3} \quad (12b)$$

$\text{cm}^{-1}/\text{mrad}$ , typically. The laser beam is constrained by apertures to have an angular wander  $<0.2$  mrad. The ion beam is constrained to about the same degree; in this case one of the "apertures" is the intersection with the laser beam. Angular wander of the ion beam was further checked with a Faraday monitor downstream from this intersection. Changes in the angle of intersection from either cause, occurring sometime in the *a-b-a* or *b-a-b* measurement sequence, would appear as a shift in the peak positions  $E_a^L$  and  $E_a^H$  and would cause rejection of the run if large enough. Small departures from the  $\theta_a = \theta_b$  condition assumed in deriving Eq. (8) can be averaged out with sufficient data. From Eq. (12b) it can be seen that the error in  $\nu_0$  arising from an inequality of these angles can be made substantially smaller by going to collinear geometry; in this case the  $\sin\theta_a$  of Eq. (12b) would be replaced by a measure of the effective ion-beam angular divergence.

Table I summarizes the values of  $\sigma(J)$  obtained from the measured wave numbers of the various hfs components  $\sigma(F, F')$ , using the hfs corrections of Jette, Lee, and Das.<sup>23</sup> Also shown are the reference numbers of the  $I_2$  lines used,<sup>30</sup> and in the last column the Lamb shifts  $\mathcal{S}$ . The standard deviation of the mean of the  $J=0$  results is  $7 \times 10^{-4} \text{ cm}^{-1}$ , and we take this as an external estimate of the error arising from the energy and angle drifts discussed above, and from the internal consistency

TABLE I. Measured values of the hfs-free wave numbers  $\sigma(J)$  and Lamb shifts  $\mathcal{S}(J)$  of the  $2s^3S_1-2p^3P_J$  transitions in  ${}^7\text{Li}^+$ .

$J$	$F \rightarrow F'$	$I_2$ line no. <sup>a</sup>		$\sigma(J)$ <sup>b</sup> ( $\text{cm}^{-1}$ )	$\mathcal{S}(J)$ ( $\text{cm}^{-1}$ )
		$a$	$b$		
0	$\frac{3}{2} \rightarrow \frac{3}{2}$	3683	3963	18 231.3032	1.2537
0	$\frac{3}{2} \rightarrow \frac{3}{2}$	3664	3986	31.3041	1.2528
0	$\frac{5}{2} \rightarrow \frac{3}{2}$	3658	3986	31.3046	1.2523
0	$\frac{5}{2} \rightarrow \frac{3}{2}$	3671	3970	31.3019	1.2550
0	$\frac{5}{2} \rightarrow \frac{3}{2}$	3671	3970	31.3013	1.2556
		Average <sup>c</sup>		31.3030(12)	1.2539(16)
1	$\frac{3}{2} \rightarrow \frac{1}{2}$	3642	3942	26.1081	1.2544
1	$\frac{3}{2} \rightarrow \frac{1}{2}$	3642	3942	26.1090	1.2535
1	$\frac{5}{2} \rightarrow \frac{3}{2}$	3634	3948	26.1076	1.2549
		Average <sup>c</sup>		26.1082(12)	1.2543(16)
2	$\frac{5}{2} \rightarrow \frac{3}{2}$	3649	3954	28.1979	1.2545
2	$\frac{5}{2} \rightarrow \frac{3}{2}$	3649	3954	28.1976	1.2548
2	$\frac{5}{2} \rightarrow \frac{3}{2}$	3664	3938	28.1983	1.2541
		Average <sup>c</sup>		28.1979(12)	1.2545(16)

<sup>a</sup> Gerstenkorn and Luc, Ref. 30.

<sup>b</sup>  $18\,200.0000 \text{ cm}^{-1}$  must be added to all except the first entry.

<sup>c</sup> Errors represent  $1\sigma$ ; their estimation is discussed in the text.

of the  $I_2$  lines. The latter is quoted in Ref. 31 as  $5 \times 10^{-4} \text{ cm}^{-1}$ ; this is good evidence that ion- and laser-beam instabilities did not introduce a large amount of scatter into the data. In arriving at a final error estimate for  $\sigma(J)$  we must also include a  $\pm 0.001 \text{ cm}^{-1}$  uncertainty in Gerstenkorn and Luc's absolute calibration.<sup>31</sup> This in some degree duplicates the  $I_2$  internal-consistency error estimate, but we prefer to state a conservative error estimate. To arrive at the Lamb shifts we must subtract the APS values for the  $2s^3S_1-2p^3P_J$  transition wave numbers; these have an uncertainty of  $\pm 0.001 \text{ cm}^{-1}$ , which we have added in quadrature. The final values of  $\mathcal{S}$  obtained for  $J=0, 1, 2$  are given in Table II. They are in excellent agreement with the results of Bacis and Berry,<sup>8</sup> and with the theoretical calculations of Ermolaev.<sup>15</sup> Note that the value of  $\mathcal{S}$  ( $2s^3S_1-2p^3P_1$ ) from Ref. 8 has been corrected for singlet-triplet mixing; this correction was discussed in Ref. 8, but was omitted as a result of an oversight.

The only  $J$ -dependent quantity which enters the Lamb-shift calculations is the anomalous-magnetic-moment term, estimated as  $0.006 \text{ cm}^{-1}$  for the  $2p^3P_1$  level. Ermolaev has not made estimates of this term for the  $2p^3P_0$  and  $2p^3P_2$  levels, and

TABLE II. Comparison of calculated and measured values of the  $2s\ ^3S_1-2p\ ^3P_J$  differential Lamb shifts  $\mathcal{S}(J)$  in  ${}^7\text{Li}^+$ .

Author	$\mathcal{S}(0)$ ( $\text{cm}^{-1}$ )	$\mathcal{S}(1)$ ( $\text{cm}^{-1}$ )	$\mathcal{S}(2)$ ( $\text{cm}^{-1}$ )
Ermolaev <sup>a</sup>		1.3160(686)	
Bacis and Berry <sup>b</sup>		1.2502(40) <sup>c</sup>	
This work	1.2539(16)	1.2543(16)	1.2545(16)

<sup>a</sup> Reference 15.<sup>b</sup> Reference 8.<sup>c</sup> Corrected from value given in Ref. 8. See the text.

his high- $Z$  theory<sup>15</sup> cannot be applied to give accurate results in the case  $Z=3$ . In comparing our three Lamb shifts, it must be noted that the Gerstenkorn and Luc calibration uncertainty does not enter independently into the shifts; thus the *differences* have an uncertainty of  $\pm 0.0010\ \text{cm}^{-1}$ . Within these limits we find no evidence of a significant  $J$  dependence of the Lamb shift.

The  $\sigma(J)$  values of Table I may be combined to give fine-structure intervals  $\Delta\sigma_{02}$  and  $\Delta\sigma_{01}$ , and these are listed in Table III. In estimating the error of these fs intervals we have used the internal consistency of the  $I_2$  lines and the external error estimate discussed above. The  $\Delta\sigma$ 's are in excellent agreement with the less-precise experimental values of Ref. 8 and with the theoretical values of APS. There is a two standard deviation discrepancy between our value of  $\Delta\sigma_{02}$  and the very precise experimental value of zu Putlitz and co-workers,<sup>14</sup> which is itself in disagreement by  $22\sigma$  with the APS value. A proposed new measurement<sup>34</sup> of the fine-structure intervals may resolve this discrepancy.

## V. CONCLUSIONS

We have demonstrated a precision method for using Doppler-tuned laser spectroscopy to measure optical-transition wave numbers to an accuracy of  $0.001\ \text{cm}^{-1}$  without the need for accurate

knowledge of the absolute ion-beam energy. Using this approach, we have measured the Lamb shifts of the  $2s\ ^3S_1-2p\ ^3P_J$  transitions in  ${}^7\text{Li}^+$  to a precision of  $0.0016\ \text{cm}^{-1}$ , and the  $2p\ ^3P$  fine-structure intervals to  $0.0012\ \text{cm}^{-1}$ . The Lamb shifts are now known to a precision about 40 times greater than existing theoretical estimates, and we hope these measurements will encourage improved calculations. The present experimental accuracy is limited principally by the absolute accuracy of the  $I_2$  wave numbers, and also by drifts in the energy and angular position of the ion beam. The former limitation could be overcome by a considerably more elaborate experiment in which the laser frequency was stabilized to an  $I_2$  absorption as at present, but calibrated against an  $I_2$ -saturated-absorption stabilized HeNe laser. Such a laser system would motivate further suppression of energy and angle shifts, which could easily be achieved by going to higher energies and collinear geometry. Future work should improve the accuracy of these  $Z=3$  measurements and extend the method to the next two members of the helium isoelectronic sequence.

## ACKNOWLEDGMENTS

We would like to acknowledge the financial support of the Natural Sciences and Engineering Council of Canada and the Academic Development Fund

TABLE III. Comparison of calculated and measured values of the  $2p\ ^3P$  fine structure in  ${}^7\text{Li}^+$ .

Author	Method	$\Delta\nu_{02}$ ( $\text{cm}^{-1}$ )	$\Delta\nu_{01}$ ( $\text{cm}^{-1}$ )
APS <sup>a</sup>	Theory	-3.1046	-5.1944
Bacis and Berry <sup>b</sup>	Hollow cathode	-3.1076(40)	-5.1974(40)
Bayer <i>et al.</i> <sup>c</sup>	Sat. absorption	-3.1028(2)	-5.1934(8)
This work	Ion beam	-3.1051(12)	-5.1948(12)

<sup>a</sup> Reference 18.<sup>b</sup> Reference 8.<sup>c</sup> Reference 14. Errors represent  $3\sigma$ .

of the University of Western Ontario. We are also grateful for the valuable technical assistance of J. Keyser, I. Schmidt, and H. Walter.

#### APPENDIX: I<sub>2</sub> LINE SHAPE

The Doppler width of an I<sub>2</sub> absorption line in the neighborhood of 18 200 cm<sup>-1</sup> is approximately 420 MHz at 20 °C. However, as a result of hfs, the observed lines have widths of about 1 GHz and are markedly asymmetric. In a recent Fourier-transform spectroscopy study of Gerstenkorn and Luc,<sup>30, 31</sup> averaging with an aperture function and a Fourier-apparatus function were used to ensure that the observed frequency of maximum absorption equalled the centroid of the hfs, given by

$$\nu = \frac{\sum_i A_i \nu_i^0}{\sum_i A_i}, \quad (\text{A1})$$

in which  $\{\nu_i^0, i=1, n\}$  are the central frequencies of the various hyperfine components ( $n=15$  for even  $J''$ , 21 for odd  $J''$ ), and the  $A_i$  are their relative absorption strengths. The centroids of some 22 000 lines were measured to an absolute accuracy of  $\pm 0.0010$  cm<sup>-1</sup>.

In our experiment the transmittance of the laser light through an I<sub>2</sub> cell was used to determine the laser frequency. Under these conditions the I<sub>2</sub> line shape is determined by the Doppler width and the hfs.<sup>35</sup> The total absorption coefficient  $k_\nu$  is defined by

$$I_\nu(l) = I_\nu(0) \exp[-(k_\nu/k_0)k_0 l], \quad (\text{A2})$$

in which  $I_\nu(l)$  is the intensity of light of frequency  $\nu$  transmitted through a cell of length  $l$ ,  $I_\nu(0)$  is the intensity of the light entering the cell, and  $k_0$  is the hypothetical maximum absorption coefficient in the absence of hfs. In the present case,

$$k_\nu/k_0 = \frac{\sum_i A_i e^{-\Delta_i^2}}{\sum_i A_i}, \quad (\text{A3})$$

where

$$\Delta_i = 2(\nu - \nu_i^0)(\ln 2)^{1/2}/\Delta \nu_D \quad (\text{A4})$$

and  $\Delta \nu_D$  is the FWHM Doppler width. The quantity  $k_0 l$  is determined from the experimentally measured transmission of the particular cell, using Eqs. (A2)–(A4).

A systematic study of the variation of I<sub>2</sub> hyperfine parameters with vibration and rotation quantum numbers has been carried out by Levenson and Schawlow.<sup>33</sup> The most drastic variation they noted was the dependence of the spin-rotation interaction constant  $C$  on  $E_{\nu'}$ , the vibrational energy of the  $B$  state. They were able to parametrize this dependence as

$$C = (\mu_I/I)[1.2 \times 10^5/(4400 - E_{\nu'}) - 12.5]$$

( $C$  is in kHz), where  $E_{\nu'}$  is in cm<sup>-1</sup> and  $\mu_I$  is the magnetic-dipole moment of the spin- $\frac{5}{2}$  <sup>127</sup>I nucleus. In the region of interest for us, the agreement between this curve and experiment is such that we can confidently assign conservative error estimates of  $\pm 5$  kHz to the predicted values of  $C$ . The electric-quadrupole coupling-constant difference  $\Delta eQq$  shows only a very slight variation throughout the entire range they studied; over the  $\nu' = 24$  to 28 region of interest in our experiment, it may be taken to have the constant value  $1928 \pm 25$  MHz. We are thus able to calculate accurately the hfs of any I<sub>2</sub> transition used in our studies. In doing so we insert the hfs constants from Levenson and Schawlow into the hyperfine Hamiltonian<sup>36</sup> and then diagonalize it to obtain the locations of the hyperfine components  $\nu_i^0$ .

For each Li<sup>+</sup> run we can calculate the Doppler width from the measured cell temperature; together with the hfs constants appropriate to the I<sub>2</sub> line used, this completely determines the function  $k_\nu/k_0$  given in Eq. (A3). The parameter  $k_0 l$  is then determined from Eq. (A2) by the requirement that the maximum theoretical absorption equal the measured value for the run. The I<sub>2</sub> line-shape function  $I_\nu(l)/I_\nu(0)$  is then completely determined, and a computer then calculates  $r$  from the half-maximum-absorption frequencies and the centroid. Such a calculation is performed for both  $r_a$  and  $r_b$ .

The  $r$  values obtained by this method are quite insensitive to the details of the hfs. If we vary  $C$  and  $\Delta eQq$  within the limits of error given above,  $r$  changes by at most 0.0015, which leads to an error in  $\nu_0$  of only 1 MHz ( $4 \times 10^{-5}$  cm<sup>-1</sup>), which is entirely negligible. The 0.2% uncertainty in the transmittance measurement leads to an even smaller contribution to the error in  $\nu_0$ .

<sup>1</sup>H. Schüler, *Naturwissenschaften* **12**, 579 (1924); *Z. Phys.* **66**, 431 (1930).

<sup>2</sup>G. Herzberg and H. R. Moore, *Can. J. Phys.* **37**, 1293 (1959).

<sup>3</sup>H. G. Berry and J. L. Subtil, *Phys. Rev. Lett.* **27**, 1103 (1971).

<sup>4</sup>A. Adler, W. Kahan, R. Novick, and T. Lucatorto, *Phys. Rev. A* **7**, 967 (1973).

<sup>5</sup>H. G. Berry, J. L. Subtil, E. H. Pinnington, H. J. Andrä, W. Wittmann, and A. Gaupp, *Phys. Rev. A* **7**, 1609 (1973).

<sup>6</sup>H. G. Berry and R. Bacis, *Phys. Rev. A* **8**, 36 (1973).

- <sup>7</sup>W. Wittman, K. Tillmann, and H. J. Andrä, Nucl. Instrum. Methods 110, 305 (1973).
- <sup>8</sup>R. Bacis and H. G. Berry, Phys. Rev. A 10, 466 (1974).
- <sup>9</sup>H. G. Berry, E. H. Pinnington, and J. L. Subtil, Phys. Rev. A 10, 1065 (1974).
- <sup>10</sup>W. Wittmann, thesis, Berlin University, 1977 (unpublished).
- <sup>11</sup>R. Knight, M. H. Prior, and H. A. Shugart, in *Atomic Physics 6: Proceedings of the Sixth International Conference on Atomic Physics, Riga, 1978*, edited by R. Damburg (Plenum, New York, 1979), p. 110.
- <sup>12</sup>B. Fan, A. Lurio, and D. Grischkowsky, Phys. Rev. Lett. 41, 1460 (1978).
- <sup>13</sup>B. Fan, D. Grischkowsky, and A. Lurio, Opt. Lett. 4, 233 (1979).
- <sup>14</sup>R. Bayer, J. Kowalski, R. Neumann, S. Noehte, H. Suhr, K. Winkler, and G. zu Putlitz, Z. Phys. A 292, 329 (1979).
- <sup>15</sup>A. M. Ermolaev, Phys. Rev. A 8, 1651 (1973); Phys. Rev. Lett. 34, 380 (1975).
- <sup>16</sup>Y. Accad, C. L. Pekeris, and B. Schiff, Phys. Rev. A 4, 516 (1971).
- <sup>17</sup>M. L. Lewis and P. H. Serafino, Phys. Rev. A 18, 867 (1978).
- <sup>18</sup>B. Schiff, Y. Accad, and C. L. Pekeris, Phys. Rev. A 8, 2272 (1973).
- <sup>19</sup>A. M. Ermolaev and M. Jones, J. Phys. B 5, L225 (1972).
- <sup>20</sup>Quoted in Refs. 6 and 16.
- <sup>21</sup>K. S. Suh and M. H. Zaidi, Proc. R. Soc. London Ser. A 291, 94 (1965).
- <sup>22</sup>Note that in order to conform with the usual hydrogenic notation we are defining  $\delta$  to be the Lamb shift of the  ${}^3S$  level relative to the  ${}^3P$  level.
- <sup>23</sup>A. N. Jette, T. Lee, and T. P. Das, Phys. Rev. A 9, 2337 (1974).
- <sup>24</sup>H. G. Berry and R. Bacis, Phys. Rev. A 19, 2464 (1979).
- <sup>25</sup>H. J. Andrä, in *Beam-Foil Spectroscopy*, edited by I. A. Sellin and D. J. Pegg (Plenum, New York, 1976), Vol. 2, p. 835.
- <sup>26</sup>W. H. Wing, G. A. Ruff, W. E. Lamb, Jr., and J. Spezeski, Phys. Rev. Lett. 36, 1488 (1976).
- <sup>27</sup>M. Dufay, M. Carré, M. L. Gaillard, G. Meunier, H. Winter, and A. Zganski, Phys. Rev. Lett. 37, 1678 (1976).
- <sup>28</sup>S. L. Kaufman, Opt. Commun. 17, 309 (1976).
- <sup>29</sup>S. D. Rosner, T. D. Gaily, and R. A. Holt, Phys. Rev. Lett. 40, 851 (1978).
- <sup>30</sup>S. Gerstenkorn and P. Luc, *Atlas du Spectre d'Absorption de la Molécule d'Iode* (Editions du CNRS, Paris, 1978).
- <sup>31</sup>S. Gerstenkorn and P. Luc, Rev. Phys. Appl. 14, 791 (1979).
- <sup>32</sup>R. A. Holt, S. D. Rosner, T. D. Gaily, and A. G. Adam (unpublished).
- <sup>33</sup>M. D. Levenson and A. L. Schawlow, Phys. Rev. A 6, 10 (1972); M. D. Levenson, Report No. 2015, Stanford University, 1971 (unpublished).
- <sup>34</sup>R. Neumann (private communication).
- <sup>35</sup>We neglect the natural linewidth, as the radiative lifetime is about 0.8  $\mu\text{sec}$  [see G. A. Capelle and H. P. Broida, J. Chem. Phys. 58, 4212 (1973)].
- <sup>36</sup>The matrix elements of the hyperfine Hamiltonian are conveniently summarized in G. R. Hanes, J. Lapierre, P. R. Bunker, and K. C. Shotton, J. Mol. Spectrosc. 39, 506 (1971).